Revista Mexicana de Astronomía y Astrofísica, **47**, 409–424 (2011)

ATMOSPHERIC AEROSOL VARIABILITY OVER THE REGION OF SAN PEDRO MÁRTIR FROM MODIS DATA

Mario R. Araiza Quijano and Irene Cruz-González

Instituto de Astronomía, Universidad Nacional Autónoma de México, Mexico

Received 2010 June 23; accepted 2011 August 15

RESUMEN

Se presenta un estudio del espesor óptico del aerosol atmosférico (AOT por sus siglas en inglés) en el sitio astronómico de San Pedro Mártir, B. C., México durante el periodo 2000–2008. Las mediciones del AOT se realizaron con el instrumento *Moderate Resolution Imaging Spectroradiometer* (MODIS), a bordo de los satélites *Aqua* y *Terra* de la NASA. Se han identificado valores característicos estacionales que muestran un comportamiento de mayor transparencia atmosférica durante el otoño. Las mejores condiciones de transparencia atmosférica ocurren durante octubre y noviembre. El comportamiento anual durante 2000–2008 del AOT de MODIS da valores promedio de 0.147 ± 0.103, 0.128 ± 0.090, 0.115 ± 0.081, 0.087 ± 0.066 en 4700, 5500, 6600 and 21300 Å, respectivamente. Utilizando estos valores promedio se analizó la dependencia del AOT con la longitud de onda, y se encontró que $\alpha_{\rm OIR} \sim 0.31 \pm 0.06$ y la relación $\tau_\lambda \sim 0.0061\lambda^{-0.31}$ para dispersión por aerosoles en el sitio de San Pedro Mártir.

ABSTRACT

A study is presented of the atmospheric aerosol optical thickness (AOT) in the astronomical site of San Pedro Mártir, B. C., Mexico, during the 2000–2008 period. The AOT measurements were made by the *Moderate Resolution Imaging Spectroradiometer* (MODIS) instrumentation, on board of the NASA *Aqua* and *Terra* satellites. Characteristic seasonal values were identified, showing a higher atmospheric transparency in autumn. The best conditions for atmospheric transparency occur in October and November. The annual behavior of MODIS AOT yields average values for SPM during the years 2000–2008 of 0.147 ± 0.103, 0.128 ± 0.090, 0.115 ± 0.081, 0.087 ± 0.066 at 4700, 5500, 6600 and 21300 Å, respectively. We used these mean values to analyze the wavelength dependence and found aerosol scattering slopes $\alpha_{\rm OIR} \sim 0.31 \pm 0.06$, and a relation $\tau_\lambda \sim 0.0061\lambda^{-0.31}$, for aerosol scattering over the San Pedro Mártir location.

Key Words: atmospheric effects — site testing

1. INTRODUCTION

Until recently, the measurements of the atmospheric opacity of aerosol were obtained on ground-based observing stations as AERONET from NASA, that has more than 100 stations distributed around the world. It is not until 2000 and 2002 that the operation of the NASA satellites *Terra* and *Aqua* started, and systematic measurements at different geographic locations of the atmospheric aerosol optical thickness (AOT), among many other parameters, were made available. The ambient AOT of different locations around the world have been obtained using these satellites and compared to AERONET data in several publications (e.g., Ichoku et al. 2002, 2004; de Meij et al. 2006; Pires, Correia, & Paixao 2007; Green, Kondragunta, & Ciren 2008; Xia et al. 2008), to study AOT variations.

The characterization of astronomical sites (e.g., Muñoz-Tuñón, Sarazin, & Vernin 2007; Schöck et al. 2007; Tapia et al. 2007) require a detailed and long term testing, in terms both of precision and variability, of a variety of characteristics includ-

ing fractional cloud cover, precipitable water vapor, long-term weather patterns, prevailing winds, atmospheric seeing and turbulence profiles, geologic activity, local climate variability, light pollution, among others. Mexico's National Astronomical Observatory (OAN) site is at San Pedro Mártir (SPM), located 31°02′40″ N and 115°28′00″ W, some 100 km east of the West Coast of Baja California, Mexico. Astronomical characterization studies of SPM since the 1980's have been reported in a dedicated volume edited by Cruz-González, Ávila, & Tapia (2003), and in a collection of progress reports: Cruz-González et al. (2004), Tapia, Cruz-González, & Ávila (2007), Tapia et al. (2007).

Among the concepts related to geophysical properties that have been recently introduced in astronomical site testing is the role played by aerosols (e.g., Varela et al. 2007; Varela et al. 2008). These authors argue that ambient aerosol content characterization in a site is important because aerosols may produce more stable condensation nuclei, delay precipitation and affect extraterrestrial radiation by extinction, absorption, diffusion and reflection.

We present a study of the optical depth of the atmospheric aerosol in the SPM astronomical site. The observation period considered corresponds to the years 2000 to 2008. The data were obtained from the *Moderate Resolution Imaging Spectroradiometer* (MODIS) instrumentation on board the NASA satellites *Aqua* and *Terra*. We studied the seasonal, monthly and annual behavior of the atmosphere aerosol optical thickness, AOT, at the wavelengths 470, 550, 660 and 2130 nm. This paper's content is as follows: In § 2 we present basic observational atmospheric solar radiation techniques; followed by a description of the satellites and instrumentation presented in § 3. The characteristics of the data are given in § 4 and the methodology is described in § 5, followed by results and analysis description in § 6. Finally, our conclusions are presented in § 7.

2. OBSERVATIONAL ATMOSPHERIC SOLAR RADIATION TECHNIQUES

Atmospheric solar radiation techniques consider both terrestrial and spatial observations. Terrestrial observations of direct radiation have been used to evaluate the optical depth τ_λ of atmospheric aerosols at different wavelengths λ of the electromagnetic spectrum, through the relation given by Iqbal (1983):

$$I(\lambda) = I_0(\lambda) e^{-\tau_\lambda m}\,, \tag{1}$$

where I_λ is the measured irradiance (W m^{-2}), $I_0(\lambda)$ is the atmospheric top irradiance (W m^{-2}), τ_λ is the optical depth (adimensional), m the air mass (adimensional) and λ is the wavelength (nm).

On the other hand, spatial observations of reflected solar radiation have been used to evaluate the optical depth τ_λ of atmospheric aerosols using sophisticated modeling (e.g., Toon & Pollack 1976). The details of the algorithm and the theoretical basis of aerosol data retrieval from the MODIS Collection 5 data base are presented in Remer et al. (2005) and Remer, Tanré, & Kaufman (2006). These authors point out that the ambient aerosol optical depth (AOD) is proportional to the aerosol total loading in the vertical column. They show that the upward reflectance (normalized solar radiance), at the top of the atmosphere (TOA), is a function of successive orders of radiation interactions, within the coupled surface-atmosphere system. The TOA angular (for θ_0, θ, and ϕ = the solar zenith, view zenith and relative azimuth angles) spectral reflectance given by $\rho_\lambda(\theta_0, \theta, \phi)$ at a wavelength λ results from the contribution of scattering of radiation within the atmosphere without interaction with the surface, known as the "atmospheric path reflectance", the reflection of radiation off the surface that is directly transmitted to the TOA ("surface function"), and the reflection of radiation from outside the sensor's field of view ("environment function"). They argue that if the environment function is neglected, the TOA angular spectral reflectance, $\rho^*_\lambda(\theta_0, \theta, \phi)$ can be approximated by (c.f. equation 8 in Remer et al. 2006):

$$\rho^*_\lambda(\theta_0, \theta, \phi) \;=\; \rho^a_\lambda(\theta_0, \theta, \phi) + \frac{F_\lambda(\theta_0) T_\lambda(\theta) \rho^s_\lambda(\theta_0, \theta, \phi)}{1 - s_\lambda \rho^s_\lambda(\theta_0, \theta, \phi)}\,, \tag{2}$$

where ρ^a_λ is the atmospheric path reflectance, F_λ is the normalized downward flux for zero surface reflectance, T_λ represents the upward total transmission into the satellite field of view, s_λ is the atmospheric back-scattering ratios, and ρ^s_λ is the angular spectral surface reflectance. They show that except for the surface reflectance, each term on the right hand side of this equation is a function of the aerosol type and loading, including aerosol optical depth (AOD) and the fine weighting (FW) of the ambient undisturbed aerosol. Assuming that a small set of aerosol types and loadings can describe the range of global aerosol, they have obtained a look-up table that contains their simulations of these aerosol conditions. The goal of their algorithm is to use this look-up table (c.f. their § 4.3) to determine the conditions that best mimic the MODIS-observed spectral reflectance ρ^m_λ, to retrieve the associated aerosol

properties (including AOD and FW). They argue that the difficulty lies in making the most appropriate assumptions about both the surface and atmospheric contributions. Remer et al. (2006) detailed in § 4.3 of their work the strategy, formulation and calibration with the AERONET data, and describe in detail the algorithm to obtain the land aerosol optical depth (AOD). They presented the surface reflectance assumptions in their § 4.4, followed by the retrieval algorithm in § 4.5. From the comparison to AERONET data they demonstrate that their algorithm is quite reliable for AOD and FW data from MODIS Collection 5.

3. SATELLITES AND INSTRUMENTATION

Detailed information on the *Terra* and *Aqua* multinational projects can be obtained at the NASA Web pages[1].

3.1. *Terra spacecraft*

The NASA satellite *Terra*, formerly known as *EOS AM-1*, carries a payload of five sensors that study interactions among Earth's atmosphere, land, oceans, life and radiant energy (heat and light). Each sensor is designed to meet a wide range of science objectives. Two of the instruments were supplied by Canada and Japan. *Terra* is in a 100-minute polar orbit 437 miles above Earth, flying in close formation with the photography satellite *Landsat 7*, which was launched in April 1999. In 2002 *Terra* was joined by a complementary satellite, *Aqua*, formerly known as *EOS PM-1*, that crosses over the equator each orbit at a later time. *Terra* circles Earth from pole to pole in an orbit that descends across the equator at 10:30 AM when cloud cover is minimal and its view of the surface is least obstructed. The orbit is perpendicular to the direction of Earth's spin.

3.2. *Terra sensors*

The sensors on *Terra* do not actively scan the surface like laser beams or microwave pulses do, rather, they work like a camera. Sunlight reflected by Earth, and heat emitted by Earth, pass through the apertures of *Terra*'s sensors. That radiant energy is focused on detectors that are sensitive to selected regions of the electromagnetic spectrum, ranging from visible to infrared light. The information produced by the detectors is transmitted down to Earth and processed by computers into images that people can interpret. *Terra* sends down as much as one terabyte of data per day.

[1] `http://terra.nasa.gov/` and `http://aqua.nasa.gov/`, respectively.

TABLE 1

AQUA AND THE A-TRAIN

Satellite	Launch
Aura	2004 July 15
Aqua	2002 May 4
Terra	1999 December 18

The formation of orbiting satellites is referred to as the *A-Train*, and the launch dates are resented in Table 1. Together, their overlapping radars are providing a more comprehensive picture of weather and climate on global Earth. The *A Train* satellites fly in low polar orbits 438 miles above Earth. They circle Earth 14 times a day. *Aqua* crosses the equator at approximately 1:30 AM and 1:30 PM, local time, about 3 hours behind *Terra*. Due to the narrow field of view of its instruments, it takes about 16 days for *Aqua* to map the entire surface of the planet.

3.3. *Aqua Science Instruments*

Each of the school-bus-sized satellite's six science instruments is designed to monitor a different part of our global plumbing system. The six instruments are:

- Atmospheric Infrared Sounder (AIRS)
- Advanced Microwave Sounding Unit (AMSU-A)
- Humidity Sounder for Brazil (HSB)
- Advanced Microwave Scanning Radiometer for EOS (AMSR-E)
- Moderate-Resolution Imaging Spectroradiometer (MODIS)
- Clouds and the Earth's Radiant Energy System (CERES)

The data obtained by all these instruments is available in a public database supported by NASA.

4. MODIS DATA

The MODIS data was obtained from the NASA public database[2]. The MODIS Aerosol Product monitors the ambient aerosol optical thickness (AOT $\equiv \tau$ in equation 1 above) over the oceans globally and over a portion of the continents.

We extracted MODIS data for the San Pedro Mártir, Baja California, Mexico geographic location,

[2] `http://modis.gsfc.nasa.gov/`.

TABLE 2

SAN PEDRO MÁRTIR AEROSOL OPTICAL THICKNESS (AOT) DATA

Source of solar radiation data:	MODIS Aerosol, NASA
Satellites:	*Aqua* and *Terra*
Instrument:	Moderate Resolution Imaging Spectroradiometer
Site:	San Pedro Mártir, Baja California, Mexico
Location:	
Latitude	31°02′40″ North
Longitude	115°28′00″ West
Elevation:	2830 m
Aerosol optical depth observations (2000–2008):	1078
Data Files:	4008
Format:	HDF
Product Files:	MOD04_ L2
Collection:	5
Parameter:	Corrected_ Optical_ Depth_ Land
Wavelengths, λ (nm):	470, 550, 660
Bandwidth $\Delta\lambda$ (nm):	20, 20, 50
Parameter:	Corrected_ Optical_ Depth_ Land_ wav2p1
Wavelength:	2130 nm
Bandwidth $\Delta\lambda$ (nm):	50
Re projection:	Geographic
Re-projected Files:	8016
Extraction Data Files:	8016

to obtain the ambient land aerosol optical thickness (AOT). Data were obtained for the period from January 2000 to December 2008 at the four spectrometer wavelengths: 470, 550, 660 and 2130 Å, since we are also interested in the wavelength dependence τ_λ. The data characteristics are presented in Table 2. The MODIS photometers channels are presented in Table 1 of Remer et al. (2006), we note that the central wavelength and bandwidth (in parenthesis) presented in their table are 466 (20), 553 (20), 646 (50) and 2119 (50) nm, which are slightly different from the ones in the MODIS Web site.

5. METHODOLOGY

In order to obtain the atmospheric optical thickness (AOT) data of the SPM site at the selected wavelengths (4700, 5500, 6600 y 21300 Å) a set of necessary data processing steps were required. The data were processed as follows.

5.1. *Data files acquisition MOD04*

The data files for the 2000–2008 period were obtained from the LAADS (Level 1 and Atmosphere Archive and Distribution System) Web site, where the location of the site and the required period is provided as input. The daily AOT data are available for retrieval but the supplied images are given in geodetic coordinates.

5.2. *Geographic re-projection*

The necessary transformation from geodetic to geographic coordinates was done using a re-projection script and was applied to each image file using the program HDFLook. The re-projected images were constructed with a resolution of 10 km × 10 km per pixel, which is the maximum possible resolution of the system. In this way, the site location can be obtained at the pixel position of the selected site.

5.3. *Data extraction of AOT (470, 550, 660 y 2130 nm)*

Using the re-projected images the final data extraction of the aerosol optical thickness, AOT, was done with another script, using the HDFLook program.

5.4. *Temporal AOT for SPM*

The data were extracted year by year to avoid errors. For the period 2000–2008 the total number

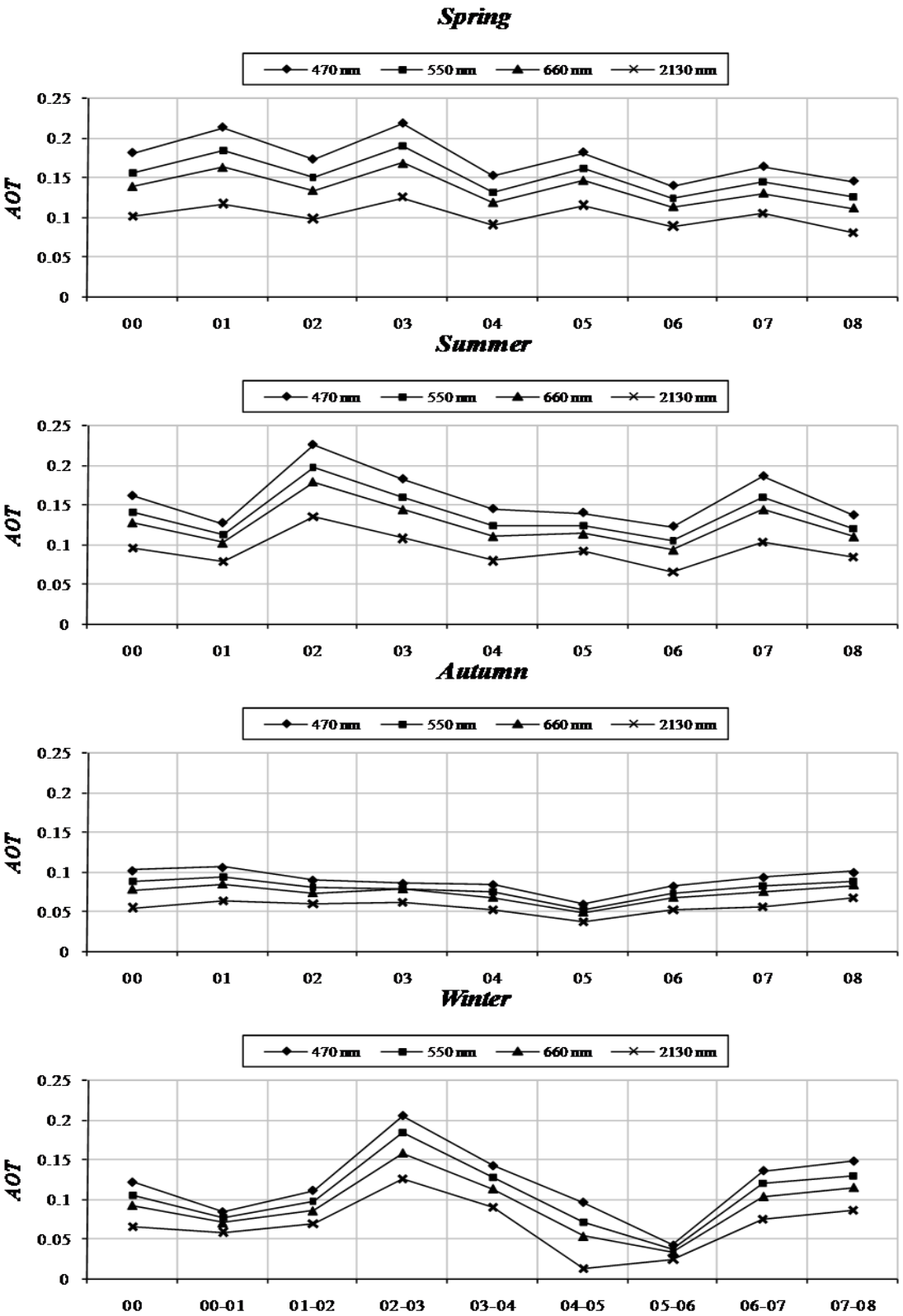

Fig. 1. The average seasonal (March to May for spring, June to August for summer, September to November for autumn, and December to February for winter) AOT above SPM over the years 2000–2008. The color figure can be viewed online.

TABLE 3

MEAN SEASONAL VARIATION OF AOT YEARLY MEASUREMENTS FOR 2000–2008

	Number of AOT Measurements				Seasonal AOT Measurement			
Year	470 nm	550 nm	660 nm	2130 nm	470 nm	550 nm	660 nm	2130 nm
					SPRING			
00	61	61	61	60	0.180 ± 0.089	0.156 ± 0.076	0.138 ± 0.068	0.101 ± 0.058
01	43	43	43	43	0.212 ± 0.084	0.183 ± 0.072	0.162 ± 0.065	0.116 ± 0.061
02	52	52	52	52	0.172 ± 0.097	0.149 ± 0.084	0.133 ± 0.075	0.097 ± 0.063
03	52	52	52	51	0.217 ± 0.134	0.188 ± 0.116	0.168 ± 0.105	0.124 ± 0.089
04	53	53	53	51	0.151 ± 0.094	0.132 ± 0.080	0.118 ± 0.071	0.090 ± 0.056
05	44	44	44	44	0.181 ± 0.121	0.161 ± 0.108	0.146 ± 0.099	0.115 ± 0.081
06	33	33	33	33	0.138 ± 0.083	0.123 ± 0.074	0.113 ± 0.068	0.089 ± 0.054
07	43	43	43	41	0.163 ± 0.089	0.144 ± 0.077	0.130 ± 0.070	0.104 ± 0.054
08	42	42	43	43	0.144 ± 0.083	0.125 ± 0.070	0.111 ± 0.060	0.081 ± 0.045
2000–2008	423	423	424	418	0.173 ±0.026	0.151 ± 0.022	0.135 ± 0.019	0.102 ± 0.014
					SUMMER			
00	29	29	29	29	0.160 ± 0.090	0.141 ± 0.080	0.127 ± 0.073	0.096 ± 0.061
01	33	33	33	33	0.126 ± 0.093	0.112 ± 0.083	0.101 ± 0.075	0.078 ± 0.061
02	49	49	50	50	0.224 ± 0.170	0.197 ± 0.154	0.178 ± 0.142	0.134 ± 0.122
03	30	30	30	30	0.181 ± 0.086	0.159 ± 0.078	0.143 ± 0.074	0.107 ± 0.066
04	44	44	44	43	0.144 ± 0.100	0.124 ± 0.083	0.109 ± 0.072	0.079 ± 0.056
05	31	31	31	30	0.139 ± 0.094	0.124 ± 0.083	0.113 ± 0.075	0.091 ± 0.059
06	29	29	29	29	0.122 ± 0.077	0.105 ± 0.064	0.092 ± 0.055	0.065 ± 0.043
07	34	34	36	36	0.185 ± 0.092	0.160 ± 0.080	0.143 ± 0.071	0.102 ± 0.064
08	34	34	34	34	0.136 ± 0.096	0.120 ± 0.084	0.109 ± 0.076	0.084 ± 0.060
2000–2008	313	313	316	314	0.157 ± 0.032	0.138 ± 0.028	0.124 ± 0.025	0.093 ± 0.019
					AUTUMN			
00	22	22	22	22	0.101 ± 0.066	0.087 ± 0.053	0.077 ± 0.046	0.055 ± 0.034
01	27	27	27	27	0.105 ± 0.062	0.093 ± 0.056	0.084 ± 0.052	0.064 ± 0.043
02	30	30	31	30	0.089 ± 0.058	0.080 ± 0.051	0.073 ± 0.046	0.060 ± 0.034
03	29	28	31	30	0.085 ± 0.079	0.078 ± 0.067	0.078 ± 0.063	0.062 ± 0.048
04	23	23	23	23	0.084 ± 0.052	0.074 ± 0.046	0.067 ± 0.042	0.052 ± 0.034
05	38	38	39	38	0.059 ± 0.062	0.052 ± 0.054	0.048 ± 0.048	0.037 ± 0.037
06	25	25	27	27	0.082 ± 0.056	0.072 ± 0.050	0.067 ± 0.045	0.052 ± 0.036
07	25	25	27	26	0.093 ± 0.068	0.081 ± 0.058	0.074 ± 0.049	0.056 ± 0.037
08	30	30	33	32	0.099 ± 0.071	0.088 ± 0.063	0.083 ± 0.055	0.067 ± 0.043
2000–2008	249	248	260	255	0.089 ± 0.013	0.078 ± 0.011	0.072 ± 0.010	0.056 ± 0.008
					WINTER			
00-01	2	2	2	2	0.084 ± 0.141	0.076 ± 0.124	0.070 ± 0.112	0.058 ± 0.085
01-02	10	10	12	11	0.111 ± 0.074	0.096 ± 0.063	0.085 ± 0.050	0.068 ± 0.037
02-03	8	8	9	9	0.205 ± 0.164	0.183 ± 0.149	0.158 ± 0.132	0.124 ± 0.110
03-04	12	12	13	13	0.142 ± 0.099	0.126 ± 0.089	0.113 ± 0.078	0.089 ± 0.063
04-05	2	2	2	2	0.096 ± 0.018	0.070 ± 0.013	0.053 ± 0.010	0.013 ± 0.002
05-06	11	11	11	11	0.041 ± 0.040	0.036 ± 0.036	0.033 ± 0.033	0.024 ± 0.027
06-07	13	13	14	14	0.135 ± 0.095	0.118 ± 0.082	0.103 ± 0.072	0.074 ± 0.061
07-08	5	5	6	6	0.147 ± 0.047	0.129 ± 0.046	0.114 ± 0.041	0.086 ± 0.040
2000–2008	63	63	69	68	0.120 ± 0.046	0.104 ± 0.042	0.091 ± 0.037	0.067 ± 0.033

of registers found was 1078, with a different number of measurements found at each wavelength.

6. RESULTS

The aerosol optical thickness for the SPM site was obtained and analyzed at the four wavelengths 4700, 5500, 6600 y 21300 Å. We explore the seasonal, monthly and annual behavior of the AOT in the 2000 to 2008 period.

6.1. *Seasonal AOT at SPM*

To study the seasonal variations of the AOT, we use the common season definition for a Northern Hemisphere location, i.e. March to May for spring, June to August for summer, September to November for autumn, and December to February for winter.

In the four panels of Figure 1 we show the seasonal behavior of the AOT at the central wavelengths

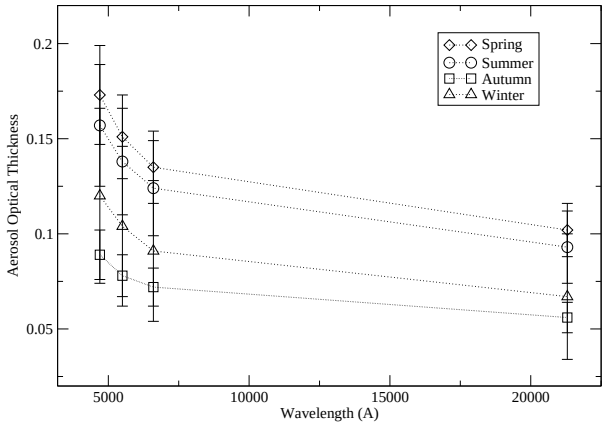

Fig. 2. The average seasonal aerosol optical depth spectral. Error bars show the estimated errors of the mean. The lowest aerosol optical thickness values occur during the autumn months.

4700, 5500, 6600 and 21300 Å. All the plots show that AOT values decrease with wavelength, as expected, and that the same variations are observed at each wavelength. In all the curves we note that the AOT is quite small, less than 0.25 for all wavelengths. In some years AOT values even less than 0.10 were obtained, specially during autumn.

In Table 3 we present the characteristics of the AOT seasonal measurements for each year during the period covered, 2000–2008, together with the resulting AOT mean values for each season and the standard deviation obtained at the four wavelengths.

By comparing the AOT values presented in Table 3 for the four seasons, we note that the lowest values are obtained in the autumn and winter months, being highest during the spring months. This is clearly seen in Figure 2 which shows the average seasonal AOT behavior with wavelength (cf. Table 3). The lowest aerosol optical thickness values occur during the autumn months with average values of 0.089 ± 0.013 at 4700 Å, 0.078 ± 0.011 at 5500 Å, 0.072 ± 0.010 at 6600 Å, and 0.056 ± 0.008 at 21300 Å. This allows us to conclude that in autumn the atmospheric transparency due to aerosols is best at SPM.

6.2. *Monthly AOT at SPM*

In Figure 3 we show the monthly behavior of the AOT at four wavelengths 470, 550, 660 and 2130 nm for the 2000 to 2008 period. For best comparison the AOT scale in all the graphs is the same. We note that in some years the months of January, February and December show scarce or no available data, while in March 2006 we found no data. The months of April to November were well covered throughout the 2000–2008 period and so the average values are more robust.

By comparing the AOT values in the twelve months we note that the lowest values are obtained in October and November, with mean values of less than 0.12 for all wavelengths. At 550 nm, which is close to the Johnson V-band, the average values in October and November are 0.074 ± 0.013 and 0.068 ± 0.021, respectively. We conclude that at all wavelengths October and November are the months with higher atmospheric transparency.

In Table 4 we present the characteristics of the AOT monthly measurements during the period 2000–2008, together with the resulting AOT average values and standard deviation.

Atmospheric extinction measurements at San Pedro Mártir have been reported by Schuster, Parrao, & Guichard (2002), and Schuster & Parrao (2001) for the years 1973–1999, and are summarized in Parrao & Schuster (2003). Individual nightly determinations of the atmospheric extinction above SPM are presented for 82 nights of 13-color photometric observations over the years 1980–1983 and from 287 nights of *ubvy* observations over the years 1984–1999. Monthly and yearly averages are given and compared for the years 1973–1999 in Schuster et al. (2002). Monthly data of atmospheric extinction above SPM covering the full period 2000–2008 are not available and so we can only compare our monthly AOT with the 1973–1999 of Schuster and collaborators. Their Tables 4, 5, and 6 show monthly averages that can be compared with our AOT mean values for the years 2000–2008.

Schuster et al. (2002) conclude that the best months for photometric observations at SPM are October and November when the atmospheric extinction is quite low, $<\kappa_y> \sim 0.1223 \pm 0.0022$ for October and 0.1195 ± 0.0022 for November, and that also during these months the observing runs are mostly stable. From their 13-color photometry they conclude that during the September, October and November months the mean observed atmospheric extinction at 5827 Å reaches the lowest values 0.1042 ± 0.0021, 0.1155 ± 0.0022 and 0.1128 ± 0.0028, respectively. These results for atmospheric extinction agree with our results for the aerosol optical depth over SPM: indeed October and November are the months with higher atmospheric transparency.

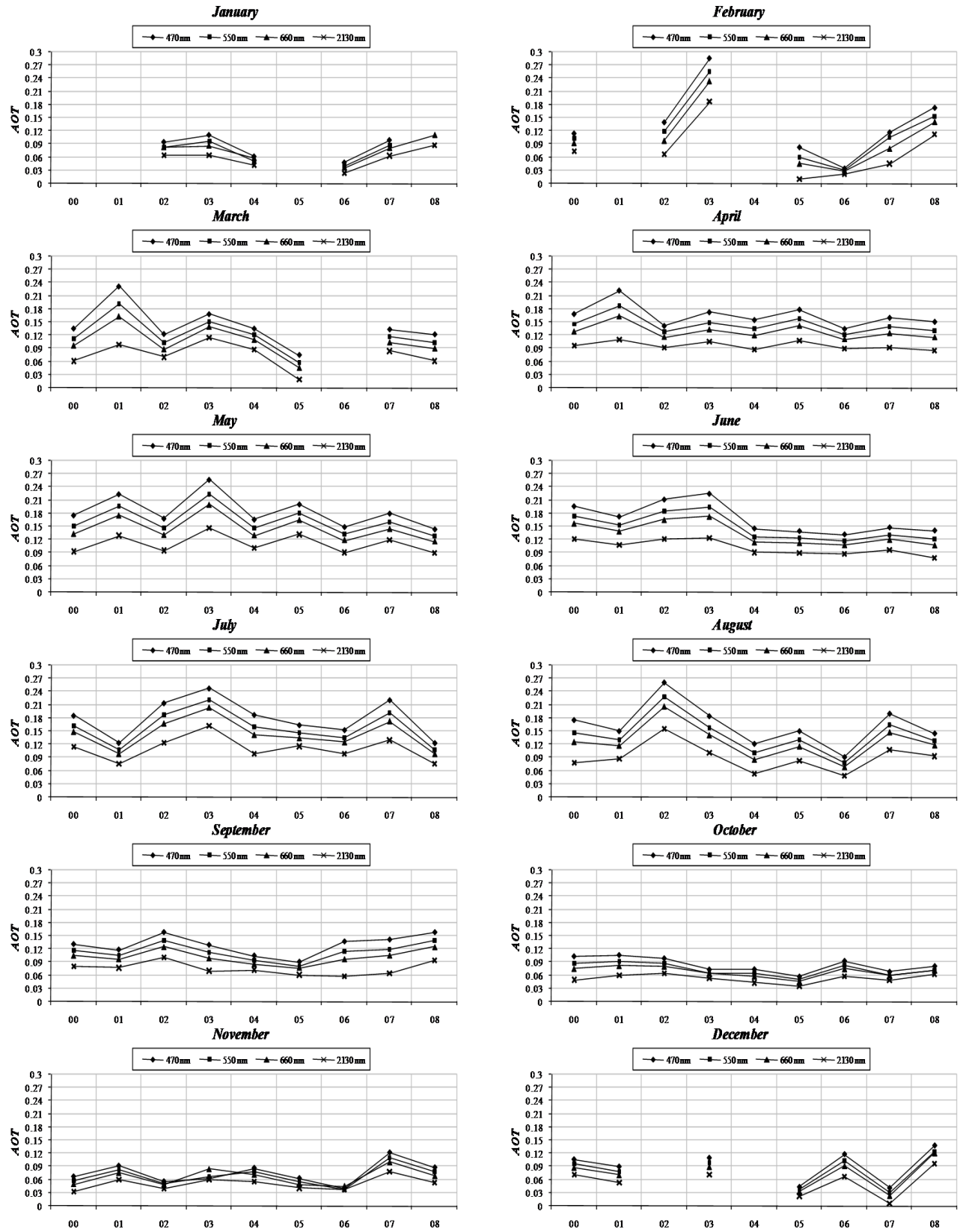

Fig. 3. Monthly Average (January to December) 2000–2008. The color figure can be viewed online.

TABLE 4

AVERAGE MONTHLY AOT ABOVE SPM OVER THE YEARS 2000–2008

	Number of AOT Measurements				Monthly AOT Measurement			
Year	470 nm	550 nm	660 nm	2130 nm	470 nm	550 nm	660 nm	2130 nm
					JANUARY			
02	3	3	4	4	0.095 ± 0.032	0.084 ± 0.029	0.083 ± 0.024	0.066 ± 0.019
03	4	4	5	5	0.111 ± 0.059	0.097 ± 0.055	0.087 ± 0.046	0.065 ± 0.041
04	3	3	4	4	0.062 ± 0.083	0.053 ± 0.073	0.058 ± 0.058	0.043 ± 0.047
06	6	6	6	6	0.048 ± 0.039	0.041 ± 0.036	0.036 ± 0.034	0.024 ± 0.030
07	1	1	1	1	0.099 ± ···	0.089 ± ···	0.081 ± ···	0.064 ± ···
08	0	0	1	1	··· ± ···	··· ± ···	0.111 ± ···	0.088 ± ···
					FEBRUARY			
00	2	2	2	2	0.115 ± 0.063	0.103 ± 0.056	0.093 ± 0.051	0.074 ± 0.040
02	5	5	6	6	0.140 ± 0.085	0.119 ± 0.072	0.098 ± 0.059	0.068 ± 0.050
03	2	2	2	2	0.286 ± 0.051	0.256 ± 0.046	0.234 ± 0.042	0.186 ± 0.035
05	1	1	1	1	0.083 ± ···	0.061 ± ···	0.046 ± ···	0.011 ± ···
06	3	3	3	3	0.035 ± 0.028	0.031 ± 0.025	0.028 ± 0.023	0.022 ± 0.018
07	1	1	2	2	0.117 ± ···	0.105 ± ···	0.080 ± 0.021	0.046 ± 0.043
08	2	2	2	2	0.173 ± 0.045	0.155 ± 0.040	0.141 ± 0.037	0.112 ± 0.029
					MARCH			
00	9	9	9	9	0.135 ± 0.072	0.113 ± 0.057	0.097 ± 0.049	0.062 ± 0.044
01	3	3	3	3	0.232 ± 0.092	0.192 ± 0.070	0.163 ± 0.060	0.099 ± 0.071
02	5	5	5	4	0.123 ± 0.083	0.103 ± 0.064	0.089 ± 0.052	0.071 ± 0.028
03	8	8	8	8	0.169 ± 0.185	0.152 ± 0.166	0.140 ± 0.152	0.114 ± 0.123
04	14	14	14	14	0.135 ± 0.089	0.121 ± 0.080	0.110 ± 0.073	0.087 ± 0.058
05	2	2	2	2	0.075 ± 0.047	0.058 ± 0.030	0.047 ± 0.019	0.020 ± 0.008
07	13	13	13	12	0.133 ± 0.103	0.116 ± 0.090	0.104 ± 0.081	0.084 ± 0.065
08	8	8	8	8	0.122 ± 0.047	0.104 ± 0.043	0.091 ± 0.041	0.062 ± 0.041
					APRIL			
00	19	19	19	18	0.169 ± 0.086	0.146 ± 0.073	0.129 ± 0.065	0.096 ± 0.054
01	14	14	14	14	0.222 ± 0.068	0.188 ± 0.059	0.164 ± 0.056	0.110 ± 0.063
02	15	15	15	15	0.142 ± 0.090	0.127 ± 0.081	0.116 ± 0.073	0.092 ± 0.058
03	11	11	11	10	0.173 ± 0.131	0.150 ± 0.111	0.133 ± 0.098	0.106 ± 0.075
04	11	11	11	11	0.155 ± 0.073	0.135 ± 0.066	0.120 ± 0.062	0.086 ± 0.058
05	19	19	19	19	0.179 ± 0.137	0.157 ± 0.121	0.142 ± 0.111	0.109 ± 0.092
06	12	12	12	12	0.135 ± 0.079	0.121 ± 0.070	0.111 ± 0.063	0.089 ± 0.048
07	14	14	14	14	0.160 ± 0.092	0.140 ± 0.076	0.125 ± 0.067	0.092 ± 0.054
08	11	11	12	12	0.151 ± 0.049	0.131 ± 0.046	0.116 ± 0.042	0.085 ± 0.043
					MAY			
00	22	22	22	22	0.176 ± 0.081	0.151 ± 0.066	0.133 ± 0.058	0.093 ± 0.053
01	16	16	16	16	0.225 ± 0.101	0.196 ± 0.087	0.175 ± 0.078	0.130 ± 0.069
02	18	18	18	18	0.169 ± 0.108	0.147 ± 0.092	0.131 ± 0.081	0.095 ± 0.065
03	20	20	20	20	0.258 ± 0.138	0.224 ± 0.123	0.200 ± 0.113	0.147 ± 0.102
04	23	23	23	22	0.167 ± 0.099	0.145 ± 0.084	0.130 ± 0.074	0.100 ± 0.057
05	18	18	18	18	0.201 ± 0.115	0.180 ± 0.103	0.165 ± 0.095	0.132 ± 0.077
06	10	10	10	10	0.150 ± 0.085	0.132 ± 0.078	0.119 ± 0.073	0.091 ± 0.064
07	14	14	14	13	0.181 ± 0.093	0.160 ± 0.083	0.144 ± 0.077	0.120 ± 0.059
08	13	13	13	13	0.145 ± 0.081	0.128 ± 0.071	0.116 ± 0.064	0.090 ± 0.049
					JUNE			
00	18	18	18	18	0.196 ± 0.102	0.174 ± 0.090	0.157 ± 0.082	0.122 ± 0.066
01	10	10	10	10	0.173 ± 0.071	0.153 ± 0.063	0.139 ± 0.057	0.109 ± 0.044
02	23	23	23	23	0.212 ± 0.119	0.185 ± 0.106	0.166 ± 0.099	0.123 ± 0.087
03	21	21	21	21	0.225 ± 0.108	0.195 ± 0.092	0.173 ± 0.083	0.124 ± 0.073
04	20	20	20	19	0.145 ± 0.100	0.127 ± 0.085	0.115 ± 0.075	0.091 ± 0.056
05	10	10	10	10	0.139 ± 0.089	0.124 ± 0.080	0.113 ± 0.073	0.090 ± 0.058
06	11	11	11	11	0.132 ± 0.093	0.118 ± 0.082	0.108 ± 0.073	0.087 ± 0.056
07	15	15	15	15	0.148 ± 0.082	0.132 ± 0.073	0.120 ± 0.067	0.096 ± 0.054
08	19	19	19	19	0.141 ± 0.104	0.122 ± 0.084	0.108 ± 0.070	0.078 ± 0.045

TABLE 4 (CONTINUED)

Year	Number of AOT Measurements				Monthly AOT Measurement			
	470 nm	550 nm	660 nm	2130 nm	470 nm	550 nm	660 nm	2130 nm
					JULY			
00	12	12	12	12	0.186 ± 0.122	0.164 ± 0.107	0.149 ± 0.097	0.114 ± 0.079
01	12	12	12	12	0.124 ± 0.066	0.109 ± 0.056	0.099 ± 0.049	0.076 ± 0.038
02	16	16	16	16	0.215 ± 0.105	0.187 ± 0.094	0.167 ± 0.087	0.124 ± 0.078
03	6	6	6	6	0.248 ± 0.118	0.222 ± 0.106	0.203 ± 0.097	0.162 ± 0.078
04	16	16	16	16	0.188 ± 0.099	0.161 ± 0.083	0.142 ± 0.074	0.099 ± 0.065
05	13	13	13	12	0.164 ± 0.101	0.147 ± 0.090	0.134 ± 0.083	0.116 ± 0.060
06	8	8	8	8	0.153 ± 0.060	0.137 ± 0.054	0.125 ± 0.049	0.099 ± 0.039
07	13	13	14	14	0.221 ± 0.100	0.194 ± 0.085	0.172 ± 0.073	0.129 ± 0.064
08	11	11	11	11	0.123 ± 0.110	0.109 ± 0.096	0.099 ± 0.086	0.076 ± 0.065
					AUGUST			
00	3	3	3	3	0.175 ± 0.067	0.147 ± 0.058	0.126 ± 0.055	0.079 ± 0.062
01	9	9	9	9	0.150 ± 0.145	0.131 ± 0.131	0.118 ± 0.121	0.088 ± 0.102
02	15	15	16	16	0.261 ± 0.248	0.229 ± 0.227	0.206 ± 0.205	0.156 ± 0.179
03	8	8	8	8	0.184 ± 0.057	0.159 ± 0.056	0.141 ± 0.056	0.101 ± 0.061
04	13	13	13	13	0.121 ± 0.114	0.101 ± 0.090	0.086 ± 0.074	0.053 ± 0.051
05	6	6	6	6	0.150 ± 0.097	0.130 ± 0.084	0.116 ± 0.075	0.084 ± 0.062
06	14	14	14	14	0.091 ± 0.075	0.079 ± 0.062	0.070 ± 0.053	0.049 ± 0.039
07	9	9	9	9	0.190 ± 0.103	0.165 ± 0.091	0.148 ± 0.083	0.109 ± 0.072
08	10	10	10	10	0.145 ± 0.100	0.130 ± 0.089	0.118 ± 0.081	0.094 ± 0.065
					SEPTEMBER			
00	18	18	18	18	0.131 ± 0.054	0.116 ± 0.049	0.105 ± 0.046	0.081 ± 0.039
01	16	16	16	16	0.118 ± 0.067	0.106 ± 0.058	0.097 ± 0.052	0.078 ± 0.040
02	17	17	17	16	0.158 ± 0.109	0.139 ± 0.095	0.125 ± 0.086	0.100 ± 0.068
03	14	14	14	14	0.129 ± 0.052	0.112 ± 0.045	0.099 ± 0.041	0.071 ± 0.038
04	14	14	14	13	0.105 ± 0.068	0.093 ± 0.061	0.085 ± 0.055	0.073 ± 0.041
05	11	11	12	12	0.090 ± 0.060	0.081 ± 0.052	0.077 ± 0.046	0.062 ± 0.036
06	9	9	9	9	0.137 ± 0.075	0.114 ± 0.058	0.097 ± 0.048	0.059 ± 0.037
07	15	15	16	16	0.141 ± 0.060	0.119 ± 0.048	0.106 ± 0.042	0.065 ± 0.037
08	11	11	11	11	0.158 ± 0.091	0.139 ± 0.080	0.125 ± 0.072	0.094 ± 0.060
					OCTOBER			
00	10	10	10	10	0.104 ± 0.067	0.087 ± 0.051	0.076 ± 0.041	0.050 ± 0.027
01	12	12	12	12	0.107 ± 0.060	0.093 ± 0.056	0.082 ± 0.053	0.060 ± 0.047
02	16	16	16	16	0.099 ± 0.052	0.089 ± 0.046	0.081 ± 0.042	0.064 ± 0.034
03	15	15	17	16	0.074 ± 0.090	0.066 ± 0.077	0.065 ± 0.065	0.054 ± 0.048
04	13	13	13	13	0.075 ± 0.047	0.065 ± 0.040	0.059 ± 0.036	0.044 ± 0.029
05	20	20	20	20	0.058 ± 0.071	0.052 ± 0.060	0.047 ± 0.053	0.036 ± 0.039
06	13	13	13	13	0.093 ± 0.046	0.083 ± 0.042	0.075 ± 0.039	0.058 ± 0.033
07	12	12	14	13	0.069 ± 0.065	0.061 ± 0.057	0.061 ± 0.050	0.049 ± 0.039
08	14	14	13	12	0.082 ± 0.068	0.073 ± 0.061	0.072 ± 0.054	0.062 ± 0.041
					NOVEMBER			
00	5	5	5	5	0.067 ± 0.088	0.057 ± 0.071	0.049 ± 0.060	0.033 ± 0.040
01	9	9	9	9	0.092 ± 0.067	0.082 ± 0.060	0.075 ± 0.054	0.060 ± 0.043
02	8	8	9	9	0.056 ± 0.055	0.051 ± 0.047	0.048 ± 0.039	0.040 ± 0.027
03	6	5	6	6	0.064 ± 0.076	0.065 ± 0.067	0.084 ± 0.086	0.061 ± 0.071
04	5	5	5	5	0.087 ± 0.033	0.078 ± 0.030	0.071 ± 0.027	0.056 ± 0.021
05	10	10	10	9	0.063 ± 0.065	0.055 ± 0.058	0.050 ± 0.053	0.041 ± 0.043
06	7	7	9	9	0.040 ± 0.040	0.036 ± 0.035	0.045 ± 0.037	0.036 ± 0.028
07	6	6	6	6	0.123 ± 0.051	0.110 ± 0.045	0.100 ± 0.042	0.079 ± 0.033
08	10	10	13	13	0.088 ± 0.047	0.078 ± 0.043	0.068 ± 0.035	0.053 ± 0.030
					DECEMBER			
00	3	3	3	3	0.106 ± 0.107	0.095 ± 0.094	0.088 ± 0.085	0.071 ± 0.064
01	2	2	2	2	0.090 ± 0.093	0.079 ± 0.081	0.071 ± 0.073	0.053 ± 0.054
03	4	4	4	4	0.110 ± 0.026	0.098 ± 0.023	0.090 ± 0.021	0.071 ± 0.016
05	7	7	7	7	0.043 ± 0.046	0.037 ± 0.039	0.032 ± 0.034	0.022 ± 0.025
06	4	4	4	4	0.118 ± 0.081	0.102 ± 0.074	0.092 ± 0.069	0.067 ± 0.059
07	1	1	1	1	0.041 ± ···	0.030 ± ···	0.023 ± ···	0.005 ± ···
08	2	2	3	3	0.138 ± 0.121	0.123 ± 0.109	0.121 ± 0.072	0.096 ± 0.056

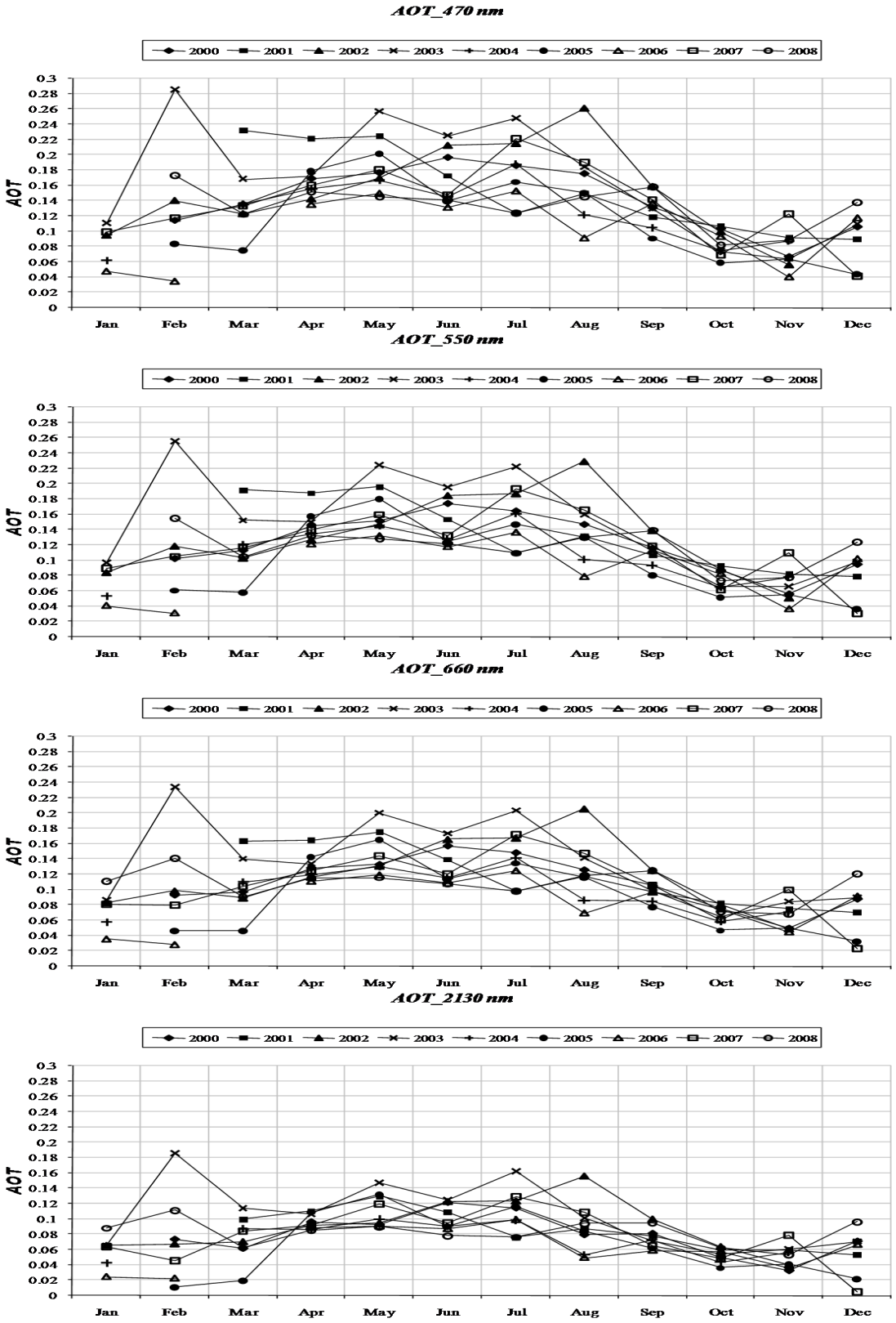

Fig. 4. Annual AOT behavior at the SPM location by monthly average at 470 nm (top), 550 nm (second from top to bottom), 660 nm (third from top to bottom), and 2130 nm (bottom). The color figure can be viewed online.

TABLE 5

AVERAGE ANNUAL AOT ABOVE SPM OVER THE YEARS 2000–2008

		Number of AOT Measurements				Annual AOT Measurement			
Year	Registers	470 nm	550 nm	660 nm	2130 nm	470 nm	550 nm	660 nm	2130 nm
2000	121	121	121	121	120	0.156 ± 0.089	0.135 ± 0.077	0.121 ± 0.069	0.088 ± 0.057
2001	103	103	103	103	103	0.157 ± 0.094	0.137 ± 0.082	0.122 ± 0.074	0.090 ± 0.061
2002	145	141	141	145	143	0.168 ± 0.131	0.147 ± 0.116	0.132 ± 0.106	0.100 ± 0.088
2003	123	119	118	122	120	0.175 ± 0.124	0.154 ± 0.108	0.138 ± 0.097	0.104 ± 0.080
2004	133	132	132	133	130	0.136 ± 0.093	0.119 ± 0.079	0.106 ± 0.070	0.079 ± 0.055
2005	118	117	117	118	116	0.126 ± 0.109	0.112 ± 0.096	0.101 ± 0.088	0.080 ± 0.071
2006	99	97	97	99	99	0.110 ± 0.076	0.097 ± 0.067	0.087 ± 0.060	0.066 ± 0.048
2007	119	114	114	119	116	0.151 ± 0.092	0.132 ± 0.080	0.118 ± 0.071	0.090 ± 0.058
2008	117	111	111	116	115	0.130 ± 0.084	0.114 ± 0.073	0.102 ± 0.063	0.078 ± 0.049
Average 2000–2008	1078	1055	1054	1076	1062	0.147 ± 0.103	0.128 ± 0.090	0.115 ± 0.081	0.087 ± 0.066

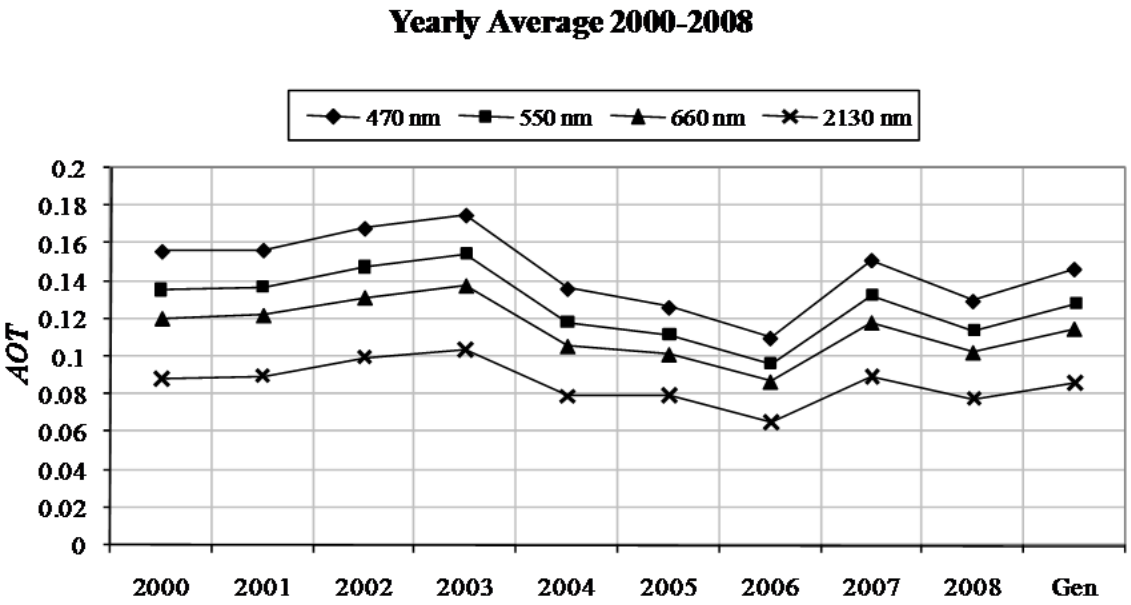

Fig. 5. Annual aerosol optical depth average at SPM at 470, 550, 660 and 2130 nm during the years 2000–2008. The color figure can be viewed online.

6.3. *Annual behavior of AOT in four wavelengths by monthly average*

In Figure 4 we show the annual behavior of the AOT by monthly average at the four wavelengths 470, 550, 660 and 2130 nm. For best comparison the AOT scale in all graphs is kept the same. By comparing the monthly AOT values we note that lowest values for the aerosol optical depth in all wavelength bands are obtained also during October and November in a consistent way through the years 2000–2008. As mentioned above, for the months of January and February there are not enough data in the studied period and mean values are less reliable.

In Table 5 we present the characteristics of the atmospheric optical depth annual measurements during the years 2000–2008 for the SPM location, together with the resulting AOT average values and standard deviation.

6.4. *Annual and general behavior of AOT*

The annual average and the general behavior of the aerosol optical depth for the SPM location for the period 2000–2008 at the four studied wavelengths 470, 550, 660 and 2130 nm is shown in Figure 5.

6.5. *AOT Climatology (2000 – 2008)*

We conclude that MODIS data obtained during the 2000–2008 of the San Pedro Mártir astronomical site in Baja California, Mexico yield an AOT climatology with the values presented in Table 6.

The final results could be compared with other sites in the globe. Gupta et al. (2006) presented

TABLE 6

SAN PEDRO MÁRTIR, BAJA CALIFORNIA (MEXICO) AEROSOL OPTICAL DEPTH CLIMATOLOGY FROM MODIS FOR 2000–2008

Wavelength (nm)	Number of AOT Measurements	AOT 2000-2008
470	1055	0.147 ± 0.103
550	1054	0.128 ± 0.090
660	1076	0.115 ± 0.081
2130	1062	0.087 ± 0.066

TABLE 7

WAVELENGTH DEPENDENCE OF SEASONAL AEROSOL OPACITY OVER SPM FROM MODIS FOR 2000–2008

Season	$\alpha_{\rm OIR}$	$\alpha_{\rm OP}$
spring	0.31 ± 0.06	0.73 ± 0.07
summer	0.31 ± 0.06	0.69 ± 0.07
autumn	0.27 ± 0.05	0.62 ± 0.11
winter	0.35 ± 0.07	0.81 ± 0.05
Average 2000–2008	0.31 ± 0.06	0.72 ± 0.08

AOT results for a collection of 26 locations in Sidney, Delhi, Hong Kong, New York City and Switzerland that cover urban populated to rural areas. The results of the rural areas in Australia and Switzerland compare quite well with the SPM results; at 550 nm they show mean annual values of 0.10 ± 0.08 and 0.16 ± 0.10, respectively, compared to our results that range from 0.10 to 0.15 in the period studied. On the other hand, Varela et al. (2008) show that in the Canarian Observatories site the AOT values found have a much wider range than the SPM values, with some dusty periods that produce a collection of MODIS AOT values at 550 nm above 0.40. But they show that, at this observatory site, most of the time the AOT have values between 0.02 and 0.20 (see Figures 12 and 13 in Varela et al. 2008). From their data in Figures 12 and 13 their average value is probably ∼0.15, reaching values as large as ∼0.7, but no average values are estimated in their work.

6.6. *AOT Spectral Slopes*

In Table 7 we present linear regression fits to the seasonal AOT values assuming that aerosols have a power-law behavior with wavelength of the form

$$AOT \equiv \tau_A(\lambda) \propto \lambda^{-\alpha}\,. \tag{3}$$

As is shown by Junge (1963) if the aerosol refractive indices are constant, aerosol particles with power-law size distributions given by $dN(r) \propto r-(\beta+1)$ produce wavelength-dependent optical depths of the form

$$\tau \propto \lambda^{-(\beta-2)}\,. \tag{4}$$

So the slope α above corresponds to the slope $\beta - 2$ of these models.

We have calculated α values, assuming $\tau_\lambda \propto \lambda^\alpha$, for the wavelengths 4700, 5500, 6600 and 21300 Å which are labeled OIR (optical to near-infrared) and for the visible region 4700, 5500 and 6600 Å labeled OP, with linear fits to the average seasonal AOT values presented in Tables 3 and 6. The results are presented in Table 7 and graphically in Figure 6. Note that $\alpha_{\rm OIR}$ has values between 0.27 (autumn) and 0.35 (winter) while $\alpha_{\rm OP}$ has values from 0.62 (autumn) to 0.82 (winter). We conclude that for periods with higher atmospheric transparency the spectral slope α is smaller and steepens for periods with higher opacity.

We have also used the average values for the years 2000–2008 (c.f. Table 6) which yield $\alpha_{\rm OIR} \sim 0.31 \pm 0.06$ ($\tau_\lambda \sim 0.0061\lambda^{-0.31}$) and $\alpha_{\rm OP} \sim 0.72 \pm 0.08$ ($\tau_\lambda \sim 0.0001\lambda^{-0.72}$) for the San Pedro Mártir location.

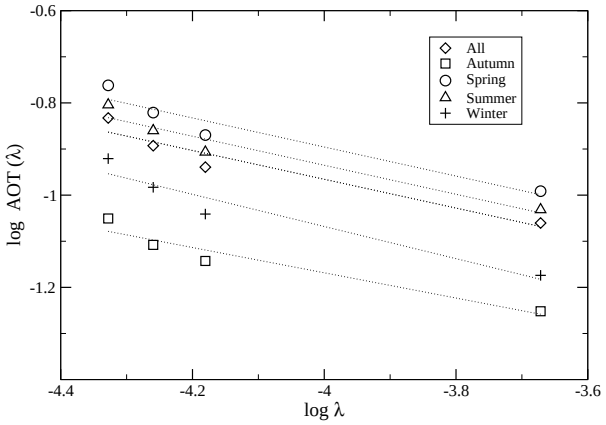

Fig. 6. Spectral dependence of aerosol optical depth obtained from MODIS data for San Pedro Mártir. Seasonal data are shown as follows: spring (circle), summer (triangle), autumn (square) and winter (plus), together with mean values for the 2000–2008 period (diamond). The dotted lines represent the linear regression fits to the data (c.f. slope values in Table 7). The color figure can be viewed online.

We can compare these α values with the radiative transfer models of global atmospheric aerosols of Toon & Pollack (1976). In particular, with their Figure 8b where the contribution of different layers of the atmosphere is shown to produce a steepening in their calculated optical depth $\tau(\lambda)$ curves in the 0.1 to 10 μm interval, with values of $\alpha \sim 0.25$ for atmosphere heights between sea-level and 3 km, while $\alpha \sim 0.67$ for the 3–6 km layer. Toon & Pollack (1976) argue that most visible spectral measurements indicate an average $\beta \approx 3 \pm 0.5$. The average values of the aerosol optical depth found for the SPM site show that $\beta_{\rm OP} \sim 2.7$ and $\beta_{\rm OIR} \sim 2.3$, which are thus consistent with expected values from these models. For the visible we derive an aerosol optical depth $\tau_\lambda = 0.0001\lambda^{-0.72}$ and for the OIR $\tau_\lambda = 0.0061\lambda^{-0.31}$ for the average values for the 2000–2008 period of AOT over San Pedro Mártir. As is shown by Toon & Pollack (1976) their global calculated aerosol optical depth spans a larger wavelength interval and it is expected that the OIR one that spans from 4300 to 21300 Å would be a better representation of the mean AOT in a site. Considering all the AOT data from MODIS we derived for the SPM site an average slope $\alpha_{\rm OIR}$ of 0.31 ± 0.06 for the mean aerosol optical depth spectral data.

6.7. *AOT and Stellar Atmospheric Extinction*

In Figure 7 spectral values of our mean and seasonal AOT from MODIS data for the years 2000–2008, are compared with the SPM average atmospheric extinction curve (κ_λ) obtained by Schuster & Parrao (2001) and Schuster et al. (2002) from stellar photometric observations for the years 1973–1999. Although τ_λ due to aerosol scattering and the atmospheric extinction κ_λ cannot be directly related, since the extinction over $3200 \lesssim \lambda \lesssim 6500$ Å has the contributions from aerosol scattering, Rayleigh-Cabannes scattering and ozone absorption (see equation 1 in Schuster & Parrao 2001, and references within), we can only check trends in the wavelength dependence.

On the other hand, Schuster & Parrao (2001) obtained for SPM a slope $\alpha_{\rm OP}$ of 0.87 ± 0.04 from their stellar photometric measurements during the years 1973–1999 for wavelengths from 0.3 to 1.1 μm. Their slope is somewhat larger than our average value of 0.72 ± 0.05 for 2000–2008, but note that our seasonal values vary from 0.62 to 0.81 (c.f. Table 7). Stellar photometry measurements have been used to derive the aerosol scattering slope at several astronomical observatories. For the European Southern Observatory at La Silla (Chile) Burki et al. (1995) obtained a value of $\alpha_{\rm OP}$ of 1.39, while for Cerro Tololo Inter-American Observatory, Chile, Gutiérrez-Moreno, Cortés, & Moreno (1982) found values of $\alpha_{\rm OP}$ varying from 0.2 to 2.6 during the years 1964–1980. Hayes & Latham (1975) summarize in their Table 1 average values from stellar observations for several observatories: Le Houga 0.89, Boyden 0.78, Lick 0.49, Cerro Tololo 0.81, and Mount Hopkins 0.84, and derived a mean value of 0.81 for night-time stellar photometry.

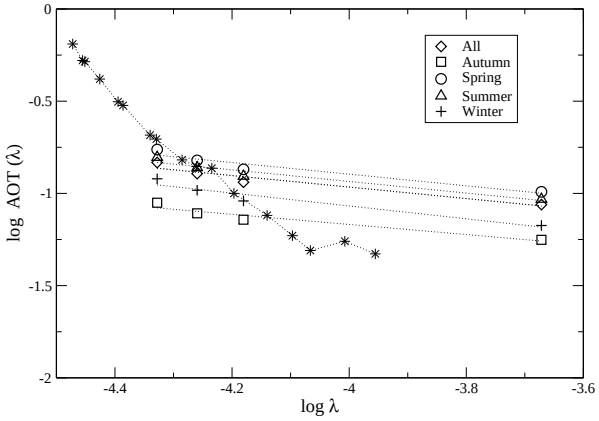

Fig. 7. Wavelength dependence of average atmospheric extinction (κ_λ) from Schuster & Parrao (2001) represented with × symbols, compared to the aerosol optical depth spectral values obtained from MODIS data for the San Pedro Mártir observatory site. The color figure can be viewed online.

If we consider the values of $\alpha_{\rm OIR}$ which probably describe somewhat better the wavelength dependence of aerosol opacity because of the larger wavelength coverage, the mean value found for SPM $\alpha_{\rm aerosol}$ of 0.31 ± 0.10 and the seasonal values 0.27 (autumn) and 0.35 (winter) compare well with the Toon & Pollack (1976) model for the atmosphere layer from 0 to 3 km, which probably indicates that at SPM this layer is dominant in the aerosol opacity.

7. CONCLUSIONS

The aerosol optical depth or thickness (AOT) values, obtained from MODIS database for the San Pedro Mártir (SPM) astronomical site in the period January 2000 to December 2008, show that the highest atmospheric transparency occurs during the autumn months, with average values AOT of 0.089 ± 0.013 at 4700 Å, 0.078 ± 0.011 at 5500 Å, 0.072 ± 0.010 at 6600 Å, and 0.056 ± 0.008 at 21300 Å. This seasonal trend is consistent with the monthly behavior that shows the best transparency conditions in October and November in all the years stud-

ied. This result agrees with Schuster et al. (2002) finding that the best months for photometric observations at SPM are October and November, when the atmospheric extinction is quite low ($<\kappa_y> \sim 0.12$) and the observing runs are mostly photometrically stable. So October and November are the months with higher atmospheric transparency and lowest atmospheric extinction.

The annual behavior of MODIS AOT during the years 2000–2008 yields mean values of 0.147 ± 0.103, 0.128 ± 0.090, 0.115 ± 0.081, 0.087 ± 0.066 at 4700, 5500, 6600 and 21300 Å, respectively.

Wavelength dependence of the aerosol optical thickness in the interval from 0.47 to 2.1 μm is analyzed for all the MODIS data assuming a power-law behavior for the aerosol scattering ($\tau_\lambda \propto \lambda^\alpha$) and indicates a slope $\alpha_{\rm OIR}$ with values between 0.27 (autumn), where the best atmospheric transparency conditions occur, and 0.35 (winter) where conditions are worse; while the 4700 to 6600 Å slope $\alpha_{\rm OP}$ has values from 0.62 (autumn) to 0.82 (winter). We conclude that for periods with higher atmospheric transparency the slope α for aerosol scattering is smaller and steepens for periods with more opacity.

We have also used the mean values for the AOT during the 2000–2008 studied period, which yields $\alpha_{\rm OIR} \sim 0.31 \pm 0.06$ ($\tau_\lambda \sim 0.0061\lambda^{-0.31}$) and $\alpha_{\rm OP} \sim 0.72 \pm 0.08$ ($\tau_\lambda \sim 0.0001\lambda^{-0.72}$) for the San Pedro Mártir location. The latter turns out to be somewhat smaller than the slope value obtained from stellar photometry by Schuster & Parrao (2001) of 0.87 for wavelengths from 0.3 to 1.1 μm. Our results confirm that the atmospheric transparency at SPM is excellent and that the best observing conditions may occur in the months of October and November.

Although we only obtained a partial climatology, since climatology requires a 20 year period, the results in the nine year period of MODIS data show that conditions over SPM are quite stable, possibly indicating that no dramatic changes in the AOT are expected. Nevertheless, further work with MODIS data is needed to obtain better estimates of the AOT, specially in the winter months of January and December, where the data are more scarce. The ambient aerosol optical thickness and the values of the aerosol spectral index of the San Pedro Mártir in Baja California astronomical site found in this paper, corroborate its high atmospheric transparency and strengthen its quality among the prime astronomical sites in the world. Finally, it is important that a long term ground-based campaign of aerosol optical depth measurements be carried out at SPM, for comparison with the MODIS AOT values obtained so far, and to establish the degree of confidence in the satellite measurements for this site.

We thank the staff at Observatorio Astronómico Nacional (Instituto de Astronomía, Universidad Nacional Autónoma de México), the Solar Radiation Observatory (Instituto de Geofísica, Universidad Nacional Autónoma de México), and the MODIS Aerosol NASA for providing valuable information and data. We thank W. Schuster and L. Parrao for kindly providing their extinction data and for helpful discussions. We also thank A. Leyva Contreras for helpful and valuable advice. We are indebted to A. Muhlia Velázquez for his assistance and personnel at the Coordination of Remote Perception in Conabio (Mexico), specially, to A. Cervera Taboada and to G. López Saldaña, for providing assistance with data processing. M. Araiza Quijano acknowledges Conacyt (Mexico) postdoctoral fellowship, and the Instituto de Astronomía, UNAM for providing the facilities and the academic environment for this work. We also thank the referee for his/her helpful comments.

REFERENCES

Burki, G., Rufener, F., Burnet, M., Richard, C., Blecha, A., & Bratschi, P. 1995, A&AS, 112, 383
Cruz-González, I., Ávila, R., & Tapia, M. 2003, RevMexAA (SC), 19, 1
Cruz-González, I., et al. 2004, Proc. SPIE, 5382, 634
de Meij, A., Krol, M., Dentener, F., Vignati, E., Cuvelier, C., & Thunis, P. 2006, Atmos. Chem. Phys., 6, 4287
Green, M. C., Kondragunta, S., & Ciren, P. 2008, Amer. Geophys. Union, Fall Meeting 2007, abst. #A24A-03
Gupta, P., Christopher, S. A., Wang, J., Gehrig, R., Lee, Y. C., & Kumar, N. 2006, Atmospheric Environment, 40, 5880
Gutiérrez-Moreno, A., Cortés, G., & Moreno, H. 1982, PASP, 94, 722
Hayes, D. S., & Latham, D. W. 1975, ApJ, 197, 593
Ichoku, C., et al. 2002, Geophys. Res. Lett., 29, MOD1-1, CiteID 8006
Ichoku, C., Kaufman, Y. J., Remer, L. A., & Levy, R. 2004, Adv. Space Res., 34, 820
Iqbal, M. 1983, An introduction to solar radiation (New York-London: Academic Press Inc.)
Junge, C. E. 1963, Air Chemistry and Radioactivity (New York: Academic Press)
Muñoz-Tuñón, C., Sarazin, M., & Vernin, J. 2007, RevMexAA (SC), 31, 1
Parrao, L., & Schuster, W. J. 2003, RevMexAA (SC), 19, 81
Pires, C., Correia, A. L., & Paixao, M. 2007, Amer. Geophys. Union, Fall Meeting 2007, abst. #A11A-0030
Remer, L. A., Tanré, D., & Kaufman, Y. J. 2006, Algorithm for Remote Sensing of Tropospheric

Aerosol from MODIS: Collection 5, NASA, Product ID: MOD04/MYD04 (http://modis.gsfc.nasa.gov/data/atbd/atbd_mod02.pdf)
Remer, L. A., et al. 2005, J. Atmospheric Sciences 62, 947
Schöck, M., Els, S., Riddle, R., Skidmore, W., & Travouillon, T. 2007, RevMexAA (SC), 31, 10
Schuster, W. J., & Parrao, L. 2001, RevMexAA, 37, 187
Schuster, W. J., Parrao, L., & Guichard, J. 2002, J. Astron. Data, 8, 2
Tapia, M., Cruz-González, I., & Avila, R. 2007, RevMexAA (SC), 28, 9
Tapia, M., Cruz-González, I., Hiriart, D., & Richer, M. 2007, RevMexAA (SC), 31, 47
Toon, O. B., & Pollack, J. B. 1976, J. Appl. Meteorology, 15, 225
Varela, A. M., Bertolin, C., Muñoz-Tuñón, C., Fuensalida, J. J., & Ortolani, S. 2007, RevMexAA (SC), 31, 106
Varela, A. M., Bertolin, C., Muñoz-Tuñón, C., Ortolani, S., & Fuensalida, J. J. 2008, MNRAS, 391, 507
Xia, X., Eck, T. F., Holben, B. N., Phillippe, G., & Chen, H. 2008, J. Geo. Res., 113, 14217

Mario R. Araiza Quijano and Irene Cruz-González: Instituto de Astronomía, Universidad Nacional Autónoma de México, Apdo. Postal 70–264, 04510 México, D. F., Mexico (maraizaq@astroscu.unam.mx, irene@astro.unam.mx).